

# Direct detection of variable tropospheric clouds near Titan's south pole

Michael E. Brown\*, Antonin H. Bouchez\* & Caitlin A. Griffith†

\* Division of Geological and Planetary Sciences, California Institute of Technology, Pasadena, California 91125, USA

† Lunar and Planetary Laboratory, University of Arizona, Tucson, Arizona 85721, USA

Atmospheric conditions on Saturn's largest satellite, Titan, allow the possibility that it could possess a methane condensation and precipitation cycle with many similarities to Earth's hydrological cycle. Detailed imaging studies<sup>1–4</sup> of Titan have hitherto shown no direct evidence for tropospheric condensation clouds, although there has been indirect spectroscopic evidence for transient clouds<sup>5,6</sup>. Here we report images and spectra of Titan that show clearly transient clouds, concentrated near the south pole, which is currently near the point of maximum solar heating. The discovery of these clouds demonstrates the existence of condensation and localized moist convection in Titan's atmosphere. Their location suggests that methane cloud formation is controlled seasonally by small variations in surface temperature, and that the clouds will move from the south to the north pole on a 15-year timescale.

Searching for clouds on Titan is best performed with high-resolution images and spectra at wavelengths between about 2.0 and 2.3  $\mu\text{m}$ . At these wavelengths, absorption of photons by Titan's methane ranges from negligible (2.00 to 2.05  $\mu\text{m}$ ) to nearly complete (2.17 to 2.29  $\mu\text{m}$ ), while absorption by Titan's haze is low<sup>5,6</sup>. The transparent range allows images at these wavelengths of the surface, while the complete range of methane absorption across the wavelength region allows spectra to probe all levels in Titan's atmosphere. High spatial resolution is necessary to recognize any small distinct cloud against the surface of Titan.

Using the adaptive optics (AO) system at the W. M. Keck observatory<sup>7</sup>, we have obtained images with both the spatial resolution and spectral coverage critical for searching for clouds. Adaptive optics achieves high spatial resolution by partially compensating for the smearing effect of turbulence in the Earth's atmosphere and delivering a near diffraction-limited image. Images from five nights of observations (Fig. 1) demonstrate the excellent spatial resolution achieved with the AO observations. Surface features which have been consistently imaged since 1995 are seen here at their highest resolution. The images from 10 and 11 December 2001 and 28 February 2002 all show almost the same face of Titan, and the reproducibility and rotation of surface features is apparent. More remarkable, however, are the transient changes visible near the south pole of Titan. These changes are more apparent in polar projections of the images (Fig. 2). The bright unresolved spot on the southern limb in the 10 and 11 December images has disappeared by February. The February image instead shows a much larger brightening extending about 1,400 km from 80° to 70° south latitude. Numerous small morphologically similar isolated bright spots occur throughout the images but cannot be verified to be transient because of a lack of duplicate coverage of most longitudes.

To determine the height in the atmosphere where the transient spots occur, we examined spectra from the 10 and 11 December bright southern spot and compared them to spectra obtained at a location 900 km directly east on the satellite, where the line-of-sight samples the same latitude at an identical zenith angle of 65° but no transient brightening occurs. A comparison between the two spectra

(Fig. 3) shows that they are essentially identical beyond 2.16  $\mu\text{m}$ . These regions of the spectrum contain strong methane absorption lines which saturate in the stratosphere of the satellite. At shorter wavelengths the methane absorption is progressively weaker, and so photons penetrate progressively deeper into the atmosphere until at a wavelength of 2.12  $\mu\text{m}$  photons reach the surface. The two spectra diverge at a wavelength of 2.155  $\mu\text{m}$ , which means that there must be a reflective layer somewhere between the stratosphere and the surface. Detailed plane-parallel radiative transfer calculations using the models of Griffith *et al.*<sup>5,6</sup> of the difference between the two spectra shows that the bright spot is best modelled as an unresolved highly reflective cloud layer with a filling factor of 25% at an altitude of  $16 \pm 5$  km above Titan's surface, in the middle of Titan's troposphere. The errors in this height estimate are dominated by uncertainties in tropospheric methane abundance; deviation from the plane-parallel assumption at this zenith angle is less than 4%. No changes are apparent in the altitude, intensity or location of the cloud from 10 to 11 December. These images and spectra conclusively demonstrate the existence of transient clouds in the troposphere of Titan and point to the presence of a vigorous and currently active cycle of methane condensation and dissipation.

The December 2001 cloud has a brightness equivalent to about 0.3% of the total brightness of the disk of Titan at these wavelengths, and can be explained by a single (foreshortened) cloud of 200 km diameter or smaller clouds with the same total area. The 28 February 2002 cloud is significantly larger, reflecting a flux equivalent to about 1% of the total flux of Titan, and covering an apparent

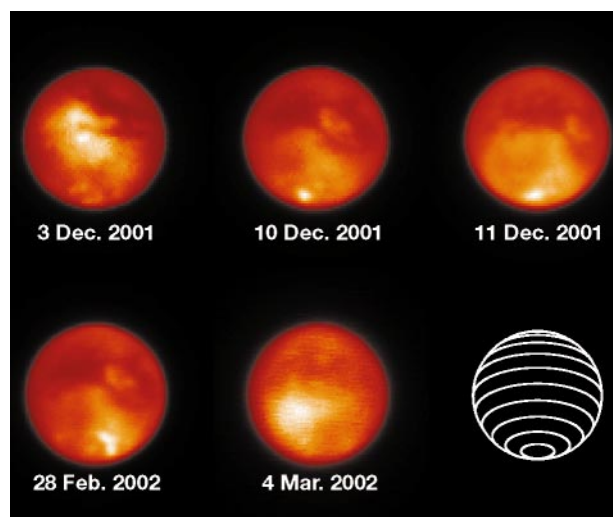


**Figure 1** Images of Titan show the transient existence of cloud features near the south pole. Images and spectra from 3, 10 and 11 December 2001 were obtained using NIRSPEC, the facility near-infrared spectrograph<sup>18</sup>, while images (only) from 28 February and 4 March 2002 were obtained using NIRC2, the facility near-infrared AO imager. Images were obtained in the K' wavelength band, which extends from 1.96 to 2.99  $\mu\text{m}$ , and have an angular resolution of 0.05 arcsec (a linear resolution of 330 km on 10 December 2001) on the satellite. The images shown are combinations of from 4 to 20 individual images shifted to a common centre, summed, and divided by an image of the individual pixel response function ('flat field'). The apparent elongation of the cloud feature on the 11 December 2001 image is a temporary artefact of the AO system. Owing to non-photometric observing conditions during some of the nights, no absolute flux calibration was obtained. The individual images are scaled to best see the polar clouds. The line figure shows every 15° of latitude projected for Titan's subsolar latitude of  $-25.6^\circ$  at the time of the observations. Titan's subsolar longitudes at the times of observations were 69°, 228°, 249°, 235° and 325° for the 3, 10 and 11 December, and the 28 February and 4 March observations, respectively.

area of  $4.4 \times 10^5 \text{ km}^2$ , which implies a filling factor of only about 5%.

These transient clouds will cause rapid changes to Titan's full-disk spectrum similar to the approximately 0.5% variations previously observed shortward of  $2.170 \mu\text{m}$  and interpreted as evidence for such clouds<sup>6</sup>. The difference in wavelength of spectral divergence between  $2.170 \mu\text{m}$  in the full-disk spectra and  $2.155 \mu\text{m}$  in the current spectra suggests a change in cloud height or latitude since the time of the previous observations.

No obvious connection exists between these transient tropospheric clouds and the southern tropopause level scattering layer<sup>8–11</sup> which occurs at an altitude of around 40 km and is visible in the spectra of Fig. 3. This layer has been observed since at least 1994 and has been described as a cloud, haze layer or fog, but its true physical nature, composition and cause remain unknown. Although this scattering layer is routinely observed, the lack of a consistent name has caused confusion as to its stability and even existence. We use the term 'tropopause cirrus' as a morphological name for this distinct layer which describes its approximate altitude, small optical depth and large areal coverage. At the time of observations, this cirrus layer covered the entire southern hemisphere at latitudes further south than  $35^\circ$  (ref. 11). The southern tropopause cirrus layer is not currently known to vary, although it is likely to change on seasonal timescales with changes in stratospheric haze chemistry and dynamics<sup>9</sup>.

The most striking property of these transient cloud events is their unexpected concentration near the south pole of Titan. Although

heating at southern summer solstice might be expected to drive polar convection, studies of tropospheric conditions on Titan have suggested an absence of seasonal variation<sup>12,13</sup> and predicted that methane clouds, if present, should concentrate at the equator year-round<sup>14</sup>. These hypothesized seasonal invariances come from consideration of the long radiative timescale of Titan's lower troposphere which does not allow tropospheric temperatures to appreciably change on seasonal timescales<sup>12</sup>.

These predictions of invariance do not consider the effects of small seasonally varying surface temperatures, however, and instead examine only conditions measured during the northern spring equinox at the time of the Voyager fly-by. Even a very small seasonally and latitudinally varying surface temperature, which is

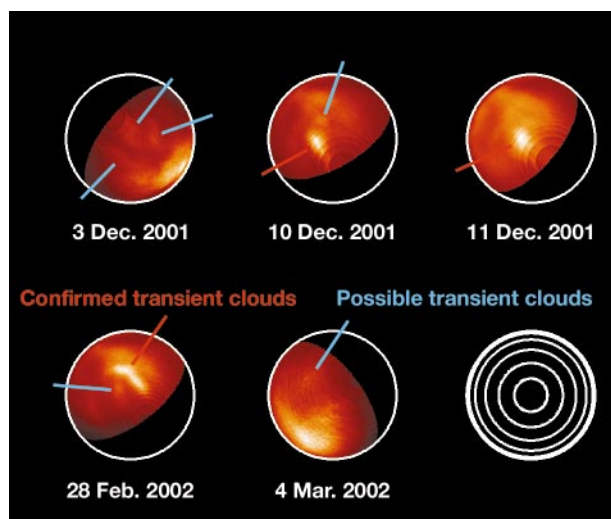


**Figure 2** The transient polar clouds are best seen in polar projections of the images of Titan. A longitude of zero (facing Saturn) is straight down in these projections and longitude increases anticlockwise. The line figure shows every  $15^\circ$  of latitude. Confirmed transients (those for which we have several images confirming change) are labelled by red lines, while morphologically similar features whose transient nature is unconfirmed are labelled by blue lines. On 10 and 11 December, the single brightest spot appears at long.  $150^\circ \pm 30^\circ$ , lat.  $77^\circ \pm 3^\circ$  south (the large errors in locating spots near the limb precludes any detection of cloud motion between the two nights). The 28 February images show small brightenings at long.  $200^\circ \pm 20^\circ$ , lat.  $87^\circ \pm 5^\circ$  south and long.  $174^\circ \pm 10^\circ$ , lat.  $65^\circ \pm 5^\circ$  south, but none at the precise location of that seen in December. Also visible is a much larger brightening between latitudes  $70^\circ$  and  $80^\circ$  south; nothing similar is seen in the December images. The projections were created by using the circular symmetry of the limb of Titan to define the centre of the disk and then projecting the intensity onto a spherical grid. Errors in the position of the centre of the disk of  $\pm 0.02$  arcsec give errors in the projected longitude and latitude of features near the south pole of  $20^\circ$  and  $5^\circ$  respectively. No intensity corrections are made for variations in the viewing angle.

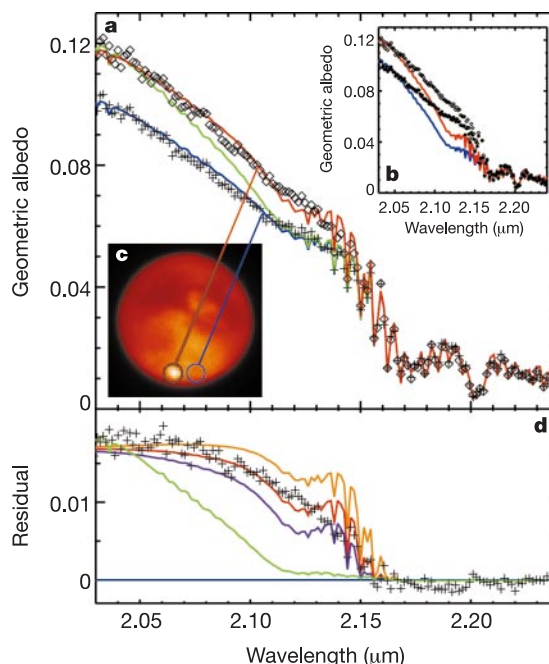


**Figure 3** Spatially resolved spectra of the disk of Titan showing the height in the atmosphere of the transient features. **a**, A comparison of a spectrum of the 10 December 2002 transient brightening and of a location 900 km east on the disk (locations shown in **c**), which samples the surface and atmosphere at an identical zenith angle of  $65^\circ$ , shows that the transient brightening is caused by tropospheric clouds. **a** compares spectra from the regions labelled on the 10 December image with best-fit radiative transfer models. The blue line shows the best-fit model to the non-cloud region, while the red line shows the effect of adding a bright scattering layer at 18 km. The green line demonstrates the poor fit obtained if an attempt is made to fit the transient brightening as a surface albedo effect. Neither spectrum can be modelled without the presence of a tropopause cirrus layer of optical depth  $0.10 \pm 0.02$  at  $2 \mu\text{m}$  at 30–40 km (refs 8–11). **b** shows the best-fit models without this tropopause cirrus. **d** shows the difference between the two spectra and between models with clouds at 14 (purple), 18 (red), and 24 km (orange). The green line again shows the poor fit if the spectral difference is modelled purely with a change in surface albedo. The mismatches between the models and data are due to inaccuracies in the methane line strengths; these inaccuracies contribute the greatest uncertainty to the derived cloud height. The spectra were obtained simultaneously using a  $0.054$  arcsecond wide spectral slit centred on the brightening and placed east–west across the disk. Both spectra have been divided by the spectrum of the G4V star HD32923 taken at an identical airmass of 1.02 to correct for effects of instrumental sensitivity, telluric absorption, and solar spectrum. The radiative transfer model uses doubling and adding techniques to approximate the equation of radiative transfer, along with line-by-line and Mie scattering calculations to incorporate gas absorption and scattering by particulates. The nominal value of methane humidity is that of ref. 6; changes of factors of two in methane or allowing methane supersaturation do not significantly change the results.

a necessary consequence of Titan's widely varying seasonal insolation, will affect the magnitude of the surface sensible heat flux and change temperatures in the lower troposphere. If the lower tropospheric lapse rate is close to the boundary between stability and instability, as has been measured on Titan<sup>13,15,16</sup>, a small additional heat flux can drive the creation of a thermally convective layer, the height of which will depend on the magnitude of the additional heat input and therefore on the surface temperature. Assuming the conditions least favourable to convection that have been inferred from Voyager measurements<sup>13</sup>, even a surface temperature rise of only 1 K is sufficient to cause a convective layer 7 km in height. If this convective layer reaches the point at which methane saturates, the height of which is highly dependent on the methane humidity but is estimated to be around 4 km in typical models<sup>6,12,15,16</sup>, methane condensation will render the air buoyant and drive clouds to the levels at about 15 km observed<sup>17</sup>. In regions with lower surface temperatures, the convective layer will be smaller or even non-existent, and condensation will not occur.

At the time of our observations, Titan was approaching southern summer solstice, and, owing to Titan's obliquity of 27°, the polar regions were in continuous sunlight and receiving more daily averaged insolation than any other spot on the satellite (and 50% more daily averaged insolation than the equator at equinox). We suggest that this insolation leads to a maximum surface temperature in these polar regions which drives a convective layer large enough to cause methane condensation and the ensuing moist convection. This hypothesis predicts that the location of these convective clouds will follow the location of maximum insolation (with some lag owing to the thermal inertia of the surface). □

Received 31 July; accepted 19 November 2002; doi:10.1038/nature01302.

1. Smith, P. H. *et al.* Titan's surface, revealed by HST imaging. *Icarus* **119**, 336–349 (1996).
2. Combes, M. *et al.* Spatially resolved images of Titan by means of adaptive optics. *Icarus* **129**, 482–497 (1997).
3. Gibbard, S. G. *et al.* Titan: High-resolution speckle images from the Keck telescope. *Icarus* **139**, 189–201 (1999).
4. Cousteins, A. *et al.* Images of Titan at 1.3 and 1.6  $\mu\text{m}$  with adaptive optics at the CFHT. *Icarus* **154**, 501–515 (2001).
5. Griffith, C. A., Owen, T., Miller, G. A. & Geballe, T. Transient clouds in Titan's lower atmosphere. *Nature* **395**, 575–578 (1998).
6. Griffith, C. A., Hall, J. L. & Geballe, T. R. Detection of daily clouds on Titan. *Science* **290**, 509–512 (2000).
7. Wizinowich, P. *et al.* Performance of the W.M. Keck Observatory natural guide star adaptive optics facility: the first year at the telescope. *Proc. SPIE* **4007**, 2–13 (2000).
8. Bouchez, A. H., Brown, M. E., Griffith, C. A. & Dekany, R. G. Spatially resolved spectroscopy of Titan's surface and atmosphere. *Bull. Am. Astron. Soc.* **32**, 1702 (2000).
9. Lorenz, R. D., Young, E. F. & Lemmon, M. T. Titan's smile and collar: HST observations of seasonal change 1994–2000. *Geophys. Res. Lett.* **28**, 4453–4456 (2001).
10. Griffith, C. A., Hall, J. L., Young, E., Cook, J. & Rannou, P. Imaging temporal changes on Titan. *Icarus* (in the press).
11. Bouchez, A. H., Brown, M. E., Neyman, C. R., Troy, M. & Dekany, R. G. Ground-based visible adaptive optics observations of Titan's atmosphere and surface. *Icarus* (submitted).
12. Hunten, D. M. *et al.* *Saturn* (eds Gehrels, T. & Matthews, M. S.) 671–759 (Univ. Arizona Press, Tucson, 1984).
13. McKay, C. P., Martin, S. C., Griffith, C. A. & Keller, R. M. Temperature lapse rate and methane in Titan's troposphere. *Icarus* **129**, 498–505 (1997).
14. Tokano, T., Neubauer, F. M., Laube, M. & McKay, C. P. Three-dimensional modeling of the tropospheric methane cycle on Titan. *Icarus* **153**, 130–147 (2001).
15. Lindal, G. F. *et al.* The atmosphere of Titan: An analysis of the Voyager 1 radio-occultation measurements. *Icarus* **53**, 348–363 (1983).
16. Lellouch, E. *et al.* Titan's atmosphere and hypothesized ocean: A reanalysis of Voyager 1 radio-occultation and IRIS 7.7- $\mu\text{m}$  data. *Icarus* **79**, 328–349 (1989).
17. Awal, M. & Lunine, J. I. Moist convective clouds in Titan's atmosphere. *Geophys. Res. Lett.* **21**, 2491–2494 (1994).
18. McLean, I. S. *et al.* The design and development of NIRSPEC: a near-infrared echelle spectrograph for the Keck II telescope. *Proc. SPIE* **3354**, 566–578 (1998).

**Acknowledgements** We thank E.J. Moyer and M.I. Richardson for conversations, D. Le Mignaut, R. Campbell, M. Konacki and J. Eisner for acquiring the NIRC2 data, and S. Hörst for many nights of monitoring Titan in the cold. This work was supported by a grant from the NSF Planetary Astronomy programme.

**Competing interests statement** The authors declare that they have no competing financial interests.

**Correspondence** and requests for materials should be addressed to M.E.B. (e-mail: mbrown@caltech.edu).

## Charge-ordered ferromagnetic phase in $\text{La}_{0.5}\text{Ca}_{0.5}\text{MnO}_3$

James C. Loudon, Neil D. Mathur & Paul A. Midgley

Department of Materials Science and Metallurgy, University of Cambridge, Pembroke Street, Cambridge CB2 3QZ, UK

Mixed-valent manganites are noted for their unusual magnetic, electronic and structural phase transitions. For example, the  $\text{La}_{1-x}\text{Ca}_x\text{MnO}_3$  phase diagram<sup>1</sup> shows that below transition temperatures in the range 100–260 K, compounds with  $0.2 < x < 0.5$  are ferromagnetic and metallic, whereas those with  $0.5 < x < 0.9$  are antiferromagnetic and charge ordered. In a narrow region around  $x = 0.5$ , these totally dissimilar ground states are thought to coexist<sup>2,3</sup>. It has been shown<sup>4</sup> that charge order and charge disorder can coexist in the related compound,  $\text{La}_{0.25}\text{Pr}_{0.375}\text{Ca}_{0.375}\text{MnO}_3$ . Here we present electron microscopy data for  $\text{La}_{0.5}\text{Ca}_{0.5}\text{MnO}_3$  that shed light on the distribution of these coexisting phases, and uncover an additional, unexpected phase. Using electron holography and Fresnel imaging, we find micrometre-sized ferromagnetic regions spanning several grains coexisting with similar-sized regions with no local magnetization. Holography shows that the ferromagnetic regions have a local magnetization of  $3.4 \pm 0.2$  Bohr magnetons per Mn atom (the spin-aligned value is  $3.5 \mu_B$  per Mn). We use electron diffraction and dark-field imaging to show that charge order exists in regions with no net magnetization and, surprisingly, can also occur in ferromagnetic regions.

Figure 1 shows the temperature dependence of the magnetization for three different compositions of polycrystalline  $\text{La}_{1-x}\text{Ca}_x\text{MnO}_3$  with a grain size of  $5 \mu\text{m}$  (produced by Praxair, Woodinville, Washington, USA). These measurements were made in a field of 1 T with a vibrating sample magnetometer. The  $x = 0.3$  compound (Fig. 1a) shows a standard paramagnetic-to-ferromagnetic phase transition at 256 K, and approaches the theoretical saturation moment of  $3.7 \mu_B$  per Mn (derived from the filling of the Mn  $d$  levels) at low temperatures (down to 10 K) as expected. The magnetization of the  $x = 0.66$  compound (Fig. 1c) shows a paramagnetic-to-antiferromagnetic phase transition at 250 K. The  $x = 0.5$  sample (from which the electron microscopy data is taken) appears to show both a paramagnetic-to-ferromagnetic transition at 233 K, and then an antiferromagnetic transition at 120 K measured on the cooling curve and 175 K on the warming curve (Fig. 1b). The large thermal hysteresis has been reported by other authors<sup>1,5</sup>, and may be an indication that charge ordering is a 'nucleation and growth' process. Below the Néel temperature, the magnetization is still higher than at room temperature, and there are two possible causes of this effect: spin canting<sup>6,7</sup>, or an inhomogeneous mixture of ferromagnetic and antiferromagnetic regions<sup>2,4</sup> within the same sample. We show here that the latter is the correct explanation.

According to the conventional models<sup>8–10</sup> for the low-temperature phase transitions in manganites, the antiferromagnetic phase is associated with a spontaneous ordering of  $\text{Mn}^{3+}$  and  $\text{Mn}^{4+}$  ions. If the room-temperature cell is indexed<sup>11</sup> as orthorhombic  $Pnma$  ( $a = 5.42 \text{ \AA}$ ,  $b = 7.65 \text{ \AA}$ ,  $c = 5.44 \text{ \AA}$ ), the lattice distortion caused by this charge ordering gives rise to extra reflections at positions  $(h + q, k, l)$  at low temperatures<sup>12</sup> in a diffraction pattern where  $q$  is the wavevector of the modulation. The wavevector has been seen to vary with both composition and temperature<sup>13</sup>, but here we consider only the commensurate phase  $q = 1/2$ . If an objective aperture is placed over one of these reflections, parts of the sample that charge order appear bright in an image.